Tetrahedron 70 (2014) 2796–2803

Contents lists available at ScienceDirect

Tetrahedron

journal homepage: www.elsevier.com/locate/tet

# Synthesis and redox behavior of 1,2-dihydro-1-oxabenz[*a*]azulen-2-ones

Shunji Ito [a,*], Shohei Yamazaki [a], Shun Kudo [a], Ryuta Sekiguchi [a], Jun Kawakami [a], Masayuki Takahashi [b], Takashi Matsuhashi [b], Kozo Toyota [b], Noboru Morita [b]

[a] *Graduate School of Science and Technology, Hirosaki University, Hirosaki 036-8561, Japan*
[b] *Department of Chemistry, Graduate School of Science, Tohoku University, Sendai 980-8578, Japan*

ARTICLE INFO

*Article history:*
Received 20 November 2013
Received in revised form 24 February 2014
Accepted 26 February 2014
Available online 5 March 2014

*Keywords:*
Coumarin analogues
Azulenes
Amphoteric redox behavior
Electrophilic substitution

ABSTRACT

Three new 1,2-dihydro-1-oxabenz[*a*]azulen-2-one derivatives, **1a** ($R^1$=H, $R^2$=Me), **1b** ($R^1$=H, $R^2$=Ph), and **1c** ($R^1$=COOEt, $R^2$=Me), have been synthesized by the reaction of 2-hydroxyazulene (**2a**) and its 1-ethoxycarbonyl derivative **2b** with ethyl acetoacetate (**3a**) or ethyl benzoylacetate (**3b**) in the presence of aluminum chloride. To our knowledge, these are the first examples of this type of compound, although the yield of the products is low in some cases. Their electronic properties were studied in detail utilizing the analyses of 1,2-dihydro-1-oxabenz[*a*]azulen-2-one derivative **1a** by the spectroscopic and voltammetric analyses. The analyses revealed that the fused α-pyrone system lowers both the HOMO and the LUMO energies, relative to those of parent azulene (**10**), but has much pronounced effect on the LUMO, consequently, leading to decrease in HOMO–LUMO gap, compared with those of **10**. These results should be attracted to the development of amphoteric redox materials. Reactivity toward electrophilic reagents was also examined by bromination and Vilsmeier–Haack formylation reactions of **1a**. To evaluate the scope of the reaction products we have examined Sonogashira cross-coupling reaction of the bromination products with trimethylsilylacetylene and conversion of the formylation product to dibromoolefin by the reaction with phosphorous ylide prepared with $CBr_4$ and $Ph_3P$. Effective extension of the π-electron system in the ethynyl products has been revealed by the spectroscopic analysis. These reaction products would be attracted to the application as a terminal group for electronic applications.


## 1. Introduction

Coumarin (2*H*-1-benzopyran-2-one) and its derivatives are one of the most important classes of heterocyclic compounds, which possess a wide range of biological activities, such as anti-clotting, anti-fungal, and anti-tumor activities (Fig. 1).[1,2] They are widely subsisted in a variety of plants in nature. Sufficient importance of the coumarin derivatives is attributed to not only their biological activities, but also their potentials as a useful scaffold for the development of advanced materials, such as photosensitizers,[3] fluorescent chemosensors,[4] organic light-emitting diodes,[5] and organic-based lasers.[6] Thus, numerous coumarin derivatives have been synthesized. Annulated coumarins are also attractive synthetic targets.[7–9]

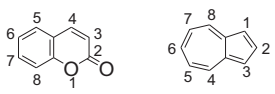


**Fig. 1.** Structure and their numbering schemes of coumarin and azulene.

Azulene ($C_{10}H_8$) has also attracted the interest of many research groups because of its unusual properties associated with its remarkable polarizability and its beautiful blue color owing to its small HOMO–LUMO gap (Fig. 1).[10] Thus, the substitution by azulenyl groups via their 1- and 3-positions promotes extreme stabilization of cationic states, while azulen-4-yl, -6-yl, and -8-yl substituents strongly stabilize anionic species. The reactivities of azulenes are also strongly affected by their polarized characters. Electrophilic substitution reactions of azulene derivatives normally induce the reaction at the 1- and 3-positions, while the nucleophilic reagents tend to induce the reaction at 4-, 6-, and 8-positions. Amphoteric redox properties of the azulene derivatives arising from their polarized natures are attractive characters that could be applied to the advanced materials for electronic applications.

During the way to explore the azulene derivatives condensed with heterocyclic rings, we have recently reported the preparation

* Corresponding author. Tel.: +81 172 39 3568; fax: +81 172 39 3541; e-mail address: itsnj@cc.hirosaki-u.ac.jp (S. Ito).

0040-4020/$ – see front matter © 2014 Elsevier Ltd. All rights reserved.
http://dx.doi.org/10.1016/j.tet.2014.02.073

of stabilized carbocations and biazulene derivative composed with thiophene-fused azulene and its derivatives.[11,12] The redox behavior of these thiophene-fused derivatives was studied in detail by voltammetric techniques. Our interests broaden the synthetic targets to the azulene analogues of coumarin derivatives possessed structural similarity consisted by the replacement of the fused benzene ring by aromatic azulene derivatives. Previously, only two examples possessing a fused structure of the α-pyrone with azulene skeleton have been examined, but in different condensation pattern from that of coumarin derivatives.[13,14] However, the azulene analogues of coumarin derivatives possessed similar condensation pattern in the α-pyrone skeleton has never been synthesized up to now, because of the lack of the useful synthetic accessibility to the best of our knowledge (Fig. 2).

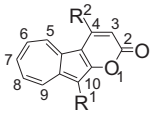


**1a**: $R^1$ = H, $R^2$ = Me
**1b**: $R^1$ = H, $R^2$ = Ph
**1c**: $R^1$ = COOEt, $R^2$ = Me

**Fig. 2.** Azulene analogues of coumarin derivatives possessed structural similarity consisted by the replacement of the fused benzene ring by aromatic azulene derivatives.

Herein, we report the synthesis of the three new 1,2-dihydro-1-oxabenz[*a*]azulen-2-one derivatives, **1a** ($R^1$=H, $R^2$=Me), **1b** ($R^1$=H, $R^2$=Ph), and **1c** ($R^1$=COOEt, $R^2$=Me), by the reaction of 2-hydroxyazulene (**2a**) and its 1-ethoxycarbonyl derivative **2b** with ethyl acetoacetate (**3a**) or ethyl benzoylacetate (**3b**) in the presence of aluminum chloride. Reactivity of **1a** toward electrophilic reagents was also examined by bromination and Vilsmeier–Haack formylation reactions, which would be attracted to the application for the further transformation of these molecular materials for electronic applications. We also report, herein, the redox properties of **1a** examined in detail by voltammetric analyses. Electronic properties of these compounds are discussed by utilizing time-dependent density functional theory (TDDFT/TDA) calculations at the B3LYP/6-31G** level. As the results, amphoteric redox properties were revealed by the 1,2-dihydro-1-oxabenz[*a*]azulen-2-one derivatives. Reactivity toward electrophilic reagents examined by bromination and Vilsmeier–Haack formylation reactions of **1a** revealed the reactive position of the 1,2-dihydro-1-oxabenz[*a*]azulene moiety. We have also examined Sonogashira cross-coupling reaction of the bromination products with trimethylsilylacetylene and conversion of the formylation product to dibromoolefin by the reaction with phosphorous ylide prepared with $CBr_4$ and $Ph_3P$. Effective extension of the π-electron system in the ethynyl products has been revealed by the spectroscopic analysis.

## 2. Results and discussion

### 2.1. Synthesis

We have applied the Pechmann condensation for the preparation of the novel 1,2-dihydro-1-oxabenz[*a*]azulen-2-one derivatives that is a powerful route for the preparation of coumarin skeleton by the reaction of β-carbonyl ester or carboxylic acid with the corresponding phenol and its derivatives under the acidic conditions.[15] The reaction of active methylene compounds with troponoid reagents, e.g., diethyl malonate with 2-methoxytropone, was well known as one of the most powerful synthetic procedures for the preparation of 2-substituted azulene derivatives.[10] The reaction of the active methylene compounds with azulene derivatives is one of the useful selections for the construction of azulene-fused hetelocycles.[16] The reaction in the presence of piperidine as a base is utilized to the preparation of azuleno[2,1-*b*]pyridine derivatives by way of the example.[17] More recently, 2-amino-3-cyano-4-aryl-10-ethoxycarbonylazuleno[2,1-*b*]pyran derivatives has been prepared by the three-component condensation of ethyl 2-hydroxyazulene-1-carboxylate, aldehydes, and malononitrile.[18] However, Pechmann condensation that should construct α-pyrone skeleton has never been examined by the reaction of 2-hydroxyazulenes with β-carbonyl ester or carboxylic acid to afford the novel 1,2-dihydro-1-oxabenz[*a*]azulen-2-one derivatives to the best of our knowledge.

Preparation of 1,2-dihydro-1-oxabenz[*a*]azulen-2-one derivatives **1a**, **1b**, and **1c** was established by the reaction of 2-hydroxyazulene (**2a**) and its 1-COOEt derivative **2b** with ethyl acetoacetate (**3a**) or ethyl benzoylacetate (**3b**) in the presence of aluminum chloride; it is outlined in Scheme 1. To our knowledge, these are the first examples of this type of compound, although the yield of the products is low in some cases. The starting materials, 2-hydroxyazulene (**2a**) and its 1-COOEt derivative **2b**, were prepared according to the literature.[19–22] The reaction of 2-hydroxyazulene (**2a**) with ethyl acetoacetate (**3a**) in the presence of aluminum chloride afforded the presumed 1,2-dihydro-4-methyl-1-oxabenz[*a*]azulen-2-one (**1a**) as brownish orange crystals in 57% yield. This procedure may have an advantage for the preparation of the novel 1,2-dihydro-1-oxabenz[*a*]azulen-2-one skeleton that may have difficulty in accessing, in one-step reaction. However, the reaction of 2-hydroxyazulene (**2a**) with ethyl benzoylacetate (**3b**) under the similar reaction conditions afforded 1,2-dihydro-1-oxa-4-phenylbenz[*a*]azulen-2-one (**1b**) as dark violet crystals, but in relatively low yield (10%). Extension of the procedure to the preparation of 10-COOEt derivative **1c** utilizing ethyl 2-hydroxyazulene-1-carboxylate (**2b**) also did not afford satisfactory results (12% yield). Thus, the procedure may have generality for the formation of 1,2-dihydro-1-oxabenz[*a*]azulen-2-one skeleton, although the yield of the products is dissatisfied in some cases. The spectral features of the 4-methyl, 4-phenyl, and 10-COOEt derivatives **1a**, **1b**, and **1c** are in agreement with the structure of the products as summarized in Experimental section.

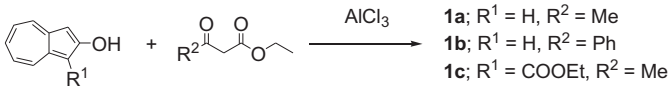


**2a**; $R^1$ = H **3a**; $R^2$ = Me
**2b**; $R^1$ = COOEt **3b**; $R^2$ = Ph

**Scheme 1.** Preparation of 1,2-dihydro-1-oxabenz[*a*]azulen-2-ones **1a**, **1b**, and **1c**.

We have now in hand novel azulene derivatives condensed with a heterocyclic ring, 1,2-dihydro-1-oxabenz[*a*]azulen-2-ones. In particularly, 4-methyl derivative **1a** could be obtained in sufficient yield for further voltammetric and chemical investigations. To obtain the aspect for the reactivities of the novel 1,2-dihydro-1-oxabenz[*a*]azulen-2-one skeleton we have firstly examined the bromination with *N*-bromosuccinimide (NBS) utilizing **1a** as a model compound. As the results, we found the two reactive positions toward the bromination in the novel 1,2-dihydro-1-oxabenz[*a*]azulen-2-one skeleton.

As expected by the azulene skeleton in the 1,2-dihydro-1-oxabenz[*a*]azulene moiety, bromination of the product **1a** utilizing NBS proceeded not only at the 10-position that corresponds the most reactive position of the azulene skeleton, but also at the 3-position. Thus, the reaction produced bromination products, 10-

bromo-1,2-dihydro-4-methyl-1-oxabenz[*a*]azulen-2-one (**4**) as yellowish brown crystals in 42% yield, along with 3,10-dibromo-1,2-dihydro-4-methyl-1-oxabenz[*a*]azulen-2-one (**5**) as brown crystals in 31% yield, when the reaction was carried with 1 equiv of NBS (Scheme 2). The increase of the amount of NBS turned the major product to **5**. Thus, the product **5** was selectively obtained by the reaction with 2 equiv of NBS in 91% yield. Thus, the reactive positions of the 1,2-dihydro-1-oxabenz[*a*]azulene moiety toward the electrophile should be concluded by the formation of the 3,10-disubstituted product.

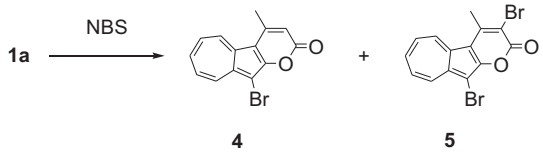


**Scheme 2.** Bromination of 1,2-dihydro-4-methyl-1-oxabenz[*a*]azulen-2-one (**1a**) with NBS.

Vilsmeier–Haack formylation might become another typical example to explore the reactivities of the novel 1,2-dihydro-1-oxabenz[*a*]azulen-2-one skeleton because of the efficiency of the reaction in azulene derivatives and also deactivate the azulene skeleton toward the multiple substitution reactions. Thus, the reaction of **1a** with phosphorous oxychloride in the presence of dimethylformamide, following the treatment with 0.1 M NaOH, was employed to obtain further aspect for the reactivity. The reaction yielded 1,2-dihydro-4-methyl-2-oxo-1-oxabenz[*a*]azulene-10-carbaldehyde (**6**) as reddish orange crystals in 78% yield (Scheme 3). These results should be concluded that there are certain differences between the two reactive positions, 3- and 10-positions. The spectral features of the mono- and dibromides **4** and **5** and carbaldehyde **6** are in agreement with the structure of the products as summarized in Experimental section.

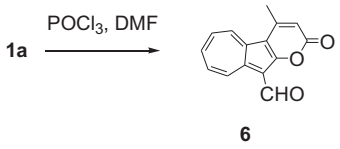


**Scheme 3.** Vilsmeier–Haack formylation of 1,2-dihydro-4-methyl-1-oxabenz[*a*]azulen-2-one (**1a**).

Reactivity of **1a** toward the electrophilic reagents would be attracted to the application for further transformation of these molecular materials for electronic applications. To evaluate the scope of the reaction products **4**, **5**, and **6** we have examined Sonogashira cross-coupling reaction of the bromination products **4** and **5** with trimethylsilylacetylene and conversion of carbaldehyde **6** to dibromoolefin by the reaction with phosphorous ylide prepared with $CBr_4$ and $Ph_3P$ to accomplish effective extension of the π-electron system.

Sonogashira cross-coupling reaction of bromide **4** with trimethylsilylacetylene was established under the palladium-catalyzed conditions at 90 °C for 24 h in a sealed-tube to afford the cross-coupled product, 1,2-dihydro-4-methyl-1-oxa-10-(trimethylsilylethynyl)benz[*a*]azulen-2-one (**7**) in 47% yield, along with the recovery of the starting **4** in 9% yield (Scheme 4). The low reactivity to the palladium-catalyzed reaction may be attributed to the high electron-density of the azulene skeleton at the 10-position in bromide **4**. We found the reaction afforded three products, when the dibromide **5** was employed to the cross-coupling reaction

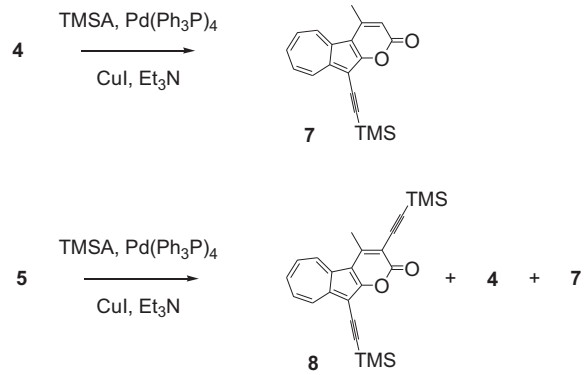


**Scheme 4.** Sonogashira cross-coupling reaction of 10-bromo- and 3,10-dibromo-1,2-dihydro-4-methyl-1-oxabenz[*a*]azulen-2-ones (**4** and **5**) with trimethylsilylacetylene.

with trimethylsilylacetylene. One is the presumed cross-coupled product, 1,2-dihydro-4-methyl-1-oxa-3,10-bis(trimethylsilylethynyl) benz[*a*]azulen-2-one (**8**), in 27% yield and the others are **4** and **7** in 6% and 53% yields, respectively (Scheme 4). Formation of **4** and **7** is attributed to the debromination at the 3-position under the cross-coupling conditions probably due to the low reactivity of **5** toward the palladium-catalyzed cross-coupling reaction.

Although low reactivity of the carbaldehyde function of **6** at the 10-position is expected due to the electron-donating nature of the azulene skeleton at this position, carbaldehyde **6** was transferred to dibromoolefin **9** in 48% yield when the reaction was carried out at 50 °C for 30 min with phosphorous ylide prepared with $CBr_4$ and $Ph_3P$ (Scheme 5). The spectral features of the ethynylated products **7** and **8** and the dibromoolefin **9** are in agreement with the structure of the products as summarized in Experimental section.

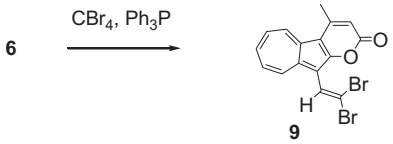


**Scheme 5.** Conversion of 1,2-dihydro-4-methyl-2-oxo-1-oxabenz[*a*]azulene-10-carbaldehyde (**6**) to dibromoolefin **9** by the reaction with phosphorous ylide prepared with $CBr_4$ and $Ph_3P$.

We have recently reported the azulene substitution at its 1-position act as an efficient terminal group for the acceleration of the reaction of acetylenes with TCNE (tetracyanoethylene) and TCNQ (tetracyanoquinodimethane) to afford azulene-substituted TCBD (tetracyanobutadiene) and DCNQ (dicyanoquinodimethane) chromophores.[23] We have also reported dibromoolefin may become a useful precursor for the enediyne scaffolds that contain multiple redox-active chromophores.[24] These reaction products may also provide the further transformation as a useful building block of these molecular materials for electronic applications.

## 2.2. Spectroscopic properties

Mass spectrum of **1a** ($R^1$=Me, $R^2$=H), **1b** ($R^1$=Ph, $R^2$=H), and **1c** ($R^1$=Me, $R^2$=COOEt) and the related products measured by ESI-TOF or MALDI-TOF conditions showed correct $M+H^+$ ion peaks, which afford a criterion of the structure of these compounds. The NMR spectra of all of the new products in $CDCl_3$ are summarized in Supplementary data, which are consisted with the structure of the products.

The typical examples of the UV and visible spectra of **1a** and the ethynylated products **7** and **8** in dichloromethane are shown in

Figs. 3 and 4, respectively, the rest is summarized in Supplementary data. The absorption spectrum of the compound **1a** is quite similar with those of its 4-phenyl and 10-COOEt derivatives **1b** and **1c** in dichloromethane although some shift of the absorption band was observed in the case of the longest wavelength absorption of 10-COOEt derivative **1c** owing to the substituted electron-withdrawing COOEt group. Compounds **1a** and **1b** showed the characteristic weak absorption of the azulene system in the visible region at $\lambda_{max}$=538 nm (log $\varepsilon$ 2.63) and $\lambda_{max}$=531 nm (log $\varepsilon$ 2.76), respectively, that should be consisted with the small HOMO–LUMO gap. The longest absorption maximum of 10-COOEt derivative **1c** in the visible region [$\lambda_{max}$=509 nm (log $\varepsilon$ 2.88)] exhibits a blue shift by 29 nm, relative to that of 10-H derivative **1a**.

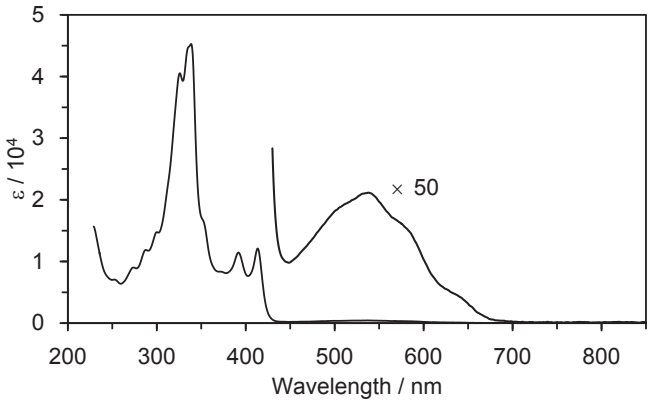


**Fig. 3.** UV/Vis spectra of 1,2-dihydro-4-methyl-1-oxabenz[*a*]azulen-2-one (**1a**) in dichloromethane.

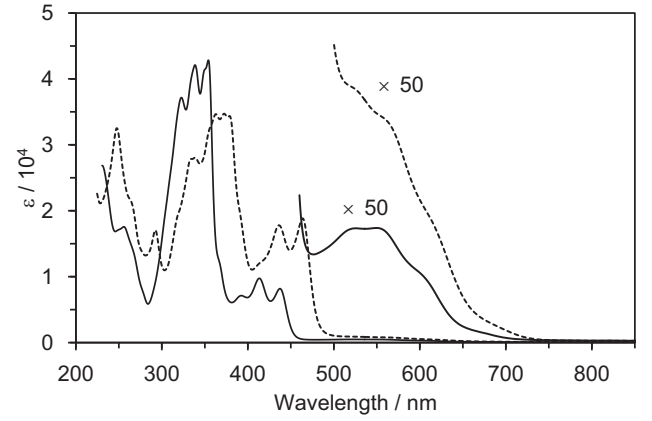


**Fig. 4.** UV/Vis spectra of the ethynyl products **7** (solid line) and **8** (dotted line) in dichloromethane.

Relative to that of parent azulene (**10**) [$\lambda_{max}$=576 nm (log $\varepsilon$ 2.51)], the longest wavelength absorption band of **1a** exhibits a blue shift by 38 nm in the same solvent.[25] The most intense band of **1a** [$\lambda_{max}$=339 nm (log $\varepsilon$ 4.66)] shows a red shift by 63 nm, compared with that of **10** [$\lambda_{max}$=276 nm (log $\varepsilon$ 4.66)]. The 1,2-dihydro-1-oxabenz[*a*]azulen-2-one series also exhibited characteristic absorption bands at around 400 nm, e.g., $\lambda_{max}$=392 nm (log $\varepsilon$ 4.06) and $\lambda_{max}$=414 nm (log $\varepsilon$ 4.08) in compound **1a**.

Effective extension of the π-electron system in the ethynyl products **7** and **8** has been revealed by the UV/Vis spectroscopic analysis. Characteristic weak absorption of the azulene system in the compounds **7** and **8** in the visible region [**7** at $\lambda_{max}$=550 nm (log $\varepsilon$ 2.54) and **8** at $\lambda_{max}$=564 sh nm (log $\varepsilon$ 2.82)] showed a distinct red shift by 12 nm and 26 nm, respectively, relative to that of **1a** that should be consisted with effective extension of the π-electron system by the substituted ethynyl groups. Furthermore, the most intense peak [**7** at $\lambda_{max}$=354 nm (log $\varepsilon$ 4.63) and **8** at $\lambda_{max}$=363 sh nm (log $\varepsilon$ 4.54)] and also characteristic absorption bands at around 400–500 nm showed similar spectral shift, compared with those of **1a**. Thus, the both trimethylsilylethynyl groups on the azulene and α-pyrone moieties effectively act as extension of the π-electron system (Fig. 4).

In contrast, introduction of the dibromoethenyl group at 10-position showed little spectral shift in the longest wavelength absorption band [**9** at $\lambda_{max}$=538 nm (log $\varepsilon$ 2.60)], relative to that of **1a**, in dichloromethane, probably due to the electron-withdrawing nature of the substituted two-bromine atoms and the less effective conjugation come from the twisted conformation of the substituent. Furthermore, the most intense peak of **9** [$\lambda_{max}$=341 nm (log $\varepsilon$ 4.63)] and also characteristic absorption bands at around 400 nm showed little spectral shift, compared with those of **1a**. The characteristic feature of the UV and visible spectra of **1a** and its related compounds was supported by TDDFT/TDA calculations at the B3LYP/6-31G** level.

### 2.3. Redox properties

To clarify the electrochemical property of the fused system, the redox behavior of **1a** was examined by cyclic voltammetry (CV) and differential pulse voltammetry (DPV) in benzonitrile containing tetraethylammonium perchlorate (0.1 M) as a supporting electrolyte. Measurements were made by using a standard three electrode configuration as platinum wire auxiliary and disk working electrodes. All measurements were carried out an argon atmosphere and potentials were related to a standard Ag/$AgNO_3$ reference electrode. Half-wave potential of ferrocene–ferrocenium couple ($Fc/Fc^+$) under the conditions using this reference electrode is observed at +0.15 V on CV.

Redox potentials (in volts vs Ag/$AgNO_3$) of **1a** along with those of azulene (**10**) itself obtained under our measurement conditions are summarized in Table 1. The CV waves of **1a** are summarized in Supplementary data. The compound **1a** exhibited an irreversible reduction wave on CV at −1.70 V. The $E_1^{red}$ wave should correspond to the one-electron injection forming a reactive radical anionic species. The oxidation of **1a** showed irreversible oxidation waves on CV at 0.91 V, 1.30 V, and 2.15 V. The irreversibility should be ascribed to the electron removal from the fused system forming a radical cationic species with high reactivity. The DPV analysis supported the existence of the three-step oxidation that should correspond to the formation of higher electronic states. The electrochemical analyses revealed the decrease of both HOMO and

**Table 1**
Redox potentials[a] of **1a** and parent azulene (**10**)[b] measured by CV and DPV

| Sample | $E_1^{red}$ [V] | $E_1^{ox}$ [V] | $E_2^{ox}$ [V] | $E_3^{ox}$ [V] |
|---|---|---|---|---|
| **1a** | (−1.70) | (+0.91) | (+1.30) | (+2.15) |
| *DPV*[c] | *−1.67* | *+0.85* | *+1.22* | *+2.03* |
| **10** | —[d] | (+0.63) | (+1.17) | |
| *DPV*[c] | *−1.95* | *+0.59* | *+1.11* | |

[a] The redox potentials were measured by CV and DPV [V versus Ag/$AgNO_3$, 1 mM in benzonitrile containing $Et_4NClO_4$ (0.1 M), Pt electrode (i.d., 1.6 mm), scan rate 100 mV $s^{-1}$, and $Fc/Fc^+$=+0.15 V]. In the case of irreversible waves on CV, which are given in parentheses, $E_{ox}$ and $E_{red}$ were calculated as $E_{pa}$ (anodic peak potential) −0.03 V and $E_{pc}$ (cathodic peak potential) +0.03 V, respectively.
[b] The redox potentials of **10** were measured under the same conditions.
[c] The values indicated by italics are peak potentials measured by DPV.
[d] The clear reduction wave could not obtained under the conditions of CV measurement.

LUMO energy levels compared with those of parent azulene (**10**), which should be attributable to the fused heterocyclic systems.

### 2.4. Theoretical calculations

To better understanding the electronic properties of the 1,2-dihydro-1-oxabenz[*a*]azulen-2-one series, we have also performed TDDFT/TDA calculations at the B3LYP/6-31G** level of 1,2-dihydro-4-methyl-1-oxabenz[*a*]azulen-2-one (**1a**) and its 10-COOMe derivative for simplification of **1c** including radical cationic and anionic species of **1a** as model compounds along with azulene (**10**) for comparative studies.[26] We have also examined the effect of the extension of the π-electron system by ethynyl and dibromoethenyl substituents on the 1,2-dihydro-1-oxabenz[*a*]azulen-2-one core utilizing the calculations at the B3LYP/6-31G** level. The results on the calculations are summarized in Supplementary data.

The calculations revealed that the fused α-pyrone system lowers both the HOMO and the LUMO energies, relative to those of parent azulene (**10**), but has much pronounced effect on the LUMO, consequently leading to slight decrease in HOMO−LUMO gap (Fig. S-26 in Supplementary data). This is affected to the amphoteric redox properties of the new system as observed by the voltammetric analyses. The TDDFT/TDA calculations reproduced the blue shift in the longest wavelength absorption band of **1a**, relative to that of parent azulene (**10**), which should be ascribed by the HOMO−LUMO+1 character in the longest wavelength absorption in addition to the HOMO−LUMO transition. Characteristic absorption bands at around 400 nm in the 1,2-dihydro-1-oxabenz[*a*]azulen-2-one series is ascribed by the theoretical calculations to be HOMO−LUMO+1 and HOMO−1−LUMO transitions, in which the molecular orbitals are also spread into the whole molecule. The blue shift in the 10-COOEt derivative **1c** should be explained by the electron-withdrawing nature of the COOEt group that should lower the HOMO energy but has less pronounced effect on the LUMO as similar with the azulene derivatives, consequently, leading to an increased HOMO−LUMO gap.

As shown in Supplementary data, the HOMO of **1a** spread into the whole molecule with the respect to the azulene nucleus and fused α-pyrone moiety, while the most of the LUMO of **1a** localized on the azulene part. Electrostatic potential map of the radical cationic species of **1a** represented to the delocalization of the most of charges on the whole molecule, while in the radical anionic species of **1a** localized the most of charges on the azulene part. Spin density also distributes on the whole molecule in the radical cationic state, whereas that of the radical anionic state mainly localizes on the azulene part. Therefore, the amphoteric redox behaviors of 1,2-dihydro-4-methyl-1-oxabenz[*a*]azulen-2-one (**1a**) are responsible to the stabilization by the fused azulene moiety.

The calculations of **7** and **8** also reproduced the extension of the π-electron system by both ethynyl groups at 3- and 10-positions, which possess large coefficient in HOMO of **1a**, but little contribution in LUMO of **1a**. The calculations revealed that the HOMO of **7** and **8** spread into both ethynyl groups at 3- and 10-positions, while the most of the LUMO of **7** and **8** localized on the 1,2-dihydro-1-oxabenz[*a*]azulen-2-one core. Thus, the π-electron system effectively extended by the both ethynyl groups at 3- and 10-positions, which lower both the HOMO and the LUMO energies, relative to those of parent **1a**, but has much pronounced effect on the HOMO, consequently, leading to decrease in HOMO−LUMO gap (Fig. S-27 in Supplementary data). The TDDFT/TDA calculations reproduced the distinct red shift in the longest wavelength absorption band of **7** and **8**, relative to that of **1a**, which should be ascribed by the HOMO−LUMO transition and also the HOMO−LUMO+1 character in **8** that should be consisted with effective extension of the π-electron system by the substituted ethynyl groups.

Two-distinct conformations were optimized with the respect to the dibromoethenyl group at 10-position. Within the structures the conformer that lean the dibromoethenyl group to the seven-membered ring side was the predominant (Fig. S-38 in Supplementary data). The twisted conformation with the dihedral angle 40° leads to the less effective conjugation between the dibromoethenyl group and the 1,2-dihydro-1-oxabenz[*a*]azulen-2-one core. The HOMO of **9** spread into the dibromoethenyl group as shown in Supplementary data that accord with the extension of the π-electron system, but less effective effect in HOMO energy in **9**, probably due to the electron-withdrawing nature of the substituted two-bromine atoms and the less effective conjugation come from the twisted conformation of the substituent, consequently, resulted to slight decrease in the HOMO−LUMO gap. The little spectral shifts in **9**, compared with those of **1a**, should be concluded to the little effect in the HOMO−LUMO gap by the dibromoethenyl substituent.

## 3. Conclusions

Three new members of 1,2-dihydro-1-oxabenz[*a*]azulen-2-one derivatives, **1a** ($R^1$=H, $R^2$=Me), **1b** ($R^1$=H, $R^2$=Ph), and **1c** ($R^1$=COOEt, $R^2$=Me) have been successfully synthesized by Lewis acid catalyzed condensation reaction of 2-hydroxyazulenes **2a** and **2b** with ethyl acetoacetate (**3a**) or ethyl benzoylacetate (**3b**). Thus, the present procedure may have generality for the formation of 1,2-dihydro-1-oxabenz[*a*]azulen-2-one skeleton, but in some cases the yield of the products is relatively low. However, 1,2-dihydro-4-methyl-1-oxabenz[*a*]azulen-2-one (**1a**) was obtained by the reaction of 2-hydroxyazulene (**2a**) with ethyl acetoacetate (**3a**) in the presence of aluminum chloride in satisfactory yield for further transformations. Thus, the reactivities of the new 1,2-dihydro-1-oxabenz[*a*]azulen-2-one derivative **1a** are revealed by the bromination utilizing NBS and Vilsmeier−Haack formylation reactions. The reactive positions of the 1,2-dihydro-1-oxabenz[*a*]azulene moiety toward the electrophiles were revealed as the 10-position that correspond to the most reactive position of azulene nucleus along with 3-position of the heterocyclic moiety that match with the reactive position of coumarin derivatives.[27] To evaluate the scope of the reaction products we have examined Sonogashira cross-coupling reaction of the bromination products **4** and **5** with trimethylsilylacetylene and conversion of the formylation product **6** to dibromoolefin **9** by the reaction with phosphorous ylide prepared with $CBr_4$ and $Ph_3P$. Thus, these reaction products would be attracted to the application as a terminal group for electronic applications.

The spectroscopic properties of 1,2-dihydro-1-oxabenz[*a*]azulen-2-one derivatives, **1a** ($R^1$=H, $R^2$=Me), **1b** ($R^1$=H, $R^2$=Ph), and **1c** ($R^1$=COOEt, $R^2$=Me) have been clarified and were compared with those of azulene (**10**) itself. As suggested by the DFT calculations, the absorption spectrum of the new members of 1,2-dihydro-1-oxabenz[*a*]azulen-2-one derivatives revealed the small HOMO−LUMO gap as similar with that of azulene (**10**) itself. The analyses revealed the decrease of both HOMO and LUMO energy levels, which should be attributable to the fused heterocyclic systems. The amphoteric redox properties observed by the electrochemical analysis of **1a** is also reflected by the small HOMO−LUMO gap of the product as similar with that of azulene (**10**) itself. Distinct red shift in the characteristic absorption bands in the visible region of the ethynyl derivatives **7** and **8**, relative to that of **1a**, is consisted with the effective extension of the π-electron system by the substituted ethynyl groups at both 3- and 10-positions.

Reactivity of **1a** toward electrophilic reagents would be attracted to the application for further transformation of these molecular materials for electronic applications. The investigation of biological activities of the new systems is a task for the future, in relation to

a wide range of biological activities of the coumarin derivatives. The synthesis of novel π-electron systems by the fusion of azulene derivatives with other heterocyclic systems are currently under investigation in our laboratory.

## 4. Experimental section

### 4.1. General

Melting points were determined on a Stuart Scientific melting point apparatus SMP3 or a Yanagimoto micro melting point apparatus MP-S3 and are uncorrected. Mass spectra were obtained with a Hitachi NanoFrontier LD instrument under ESI conditions or a Bruker Daltonics autoflex III TOF/TOF instrument under MALDI-TOF conditions. IR and UV spectra were measured on a JUSCO FT/IR-6100 or a Varian 670-IR and a JASCO V-670 spectrophotometers, respectively. $^1$H NMR spectra ($^{13}$C NMR spectra) were recorded on a JEOL ECA500 spectrometer at 500 MHz (125 MHz). $^1$H NMR chemical shifts in $CDCl_3$ are reported in parts per million (ppm) downfield from tetramethylsilane. $^{13}$C NMR chemical shifts in $CDCl_3$ are referred by the solvent signals at 77.0 ppm. The peak assignment of $^1$H and $^{13}$C NMR spectra reported was accomplished by HH COSY, DEPT, HMQC, and HMBC experiments. Elemental analyses were performed at the Instrumental Analysis Center of Hirosaki University. The voltammetry measurements were carried out in benzonitrile containing $Et_4NClO_4$ (0.1 M) as a supporting electrolyte utilizing Pt working and auxiliary electrodes, and a reference electrode formed from $Ag/AgNO_3$ (0.01 M) in acetonitrile containing *n*-$Bu_4NClO_4$ (0.1 M) at the scan rate of 100 mV s$^{-1}$. The internal reference $Fc/Fc^+$ discharges at +0.15 V under these conditions.

*4.1.1. 1,2-Dihydro-4-methyl-1-oxabenz[a]azulen-2-one (**1a**).* A solution of 2-hydroxyazulene (**2a**) (502 mg, 3.48 mmol) and ethyl acetoacetate (**3a**) (491 mg, 3.77 mmol) in 1,2-dichloroethane (50 mL) was refluxed for 15 h in the presence of aluminum chloride (1.00 g, 7.50 mmol). The reaction mixture was poured into 2 M HCl solution and extracted with dichloromethane. The organic layer was washed with brine, dried over $MgSO_4$, and concentrated under reduced pressure. The residue was purified by column chromatography on silica gel with ethyl acetate/hexane (1:4) to afford **1a** (419 mg, 57%). Brownish orange crystals; mp 168.0–170.0 °C (toluene); $^1$H NMR (500 MHz, $CDCl_3$): $\delta$=8.70 (d, 1H, *J*=9.3 Hz, 5-H), 8.35 (d, 1H, *J*=9.7 Hz, 9-H), 7.69 (dd, 1H, *J*=9.6, 9.3 Hz, 7-H), 7.45 (dd, 1H, *J*=9.6, 9.3 Hz, 6-H), 7.41 (dd, 1H, *J*=9.7, 9.3 Hz, 8-H), 7.08 (s, 1H, 10-H), 6.03 (s, 1H, 3-H), 2.77 (s, 3H, 4-Me); $^{13}$C NMR (125 MHz, $CDCl_3$): $\delta$=162.65 (C-10a), 162.32 (C-2), 152.21 (C-4), 142.41 (C-9a), 136.80 (C-9), 136.59 (C-7), 134.66 (C-4b), 133.69 (C-5), 127.25 (C-8), 126.86 (C-6), 109.12 (C-4a), 108.90 (C-3), 103.81 (C-10), 21.88 (4-Me); IR (KBr disk): $\nu_{max}$=3102 (w), 2972 (w), 1699 (s), 1593 (w), 1569 (m), 1517 (s), 1481 (w), 1450 (m), 1397 (m), 1368 (w), 1308 (w), 1280 (w), 1204 (w), 1173 (w), 1058 (w), 1043 (w), 1020 (w), 935 (w), 914 (w), 878 (m), 820 (w), 787 (m), 752 (w), 729 (m), 675 (w), 621 (w), 599 (w), 576 (w), 537 (w) cm$^{-1}$; UV/Vis ($CH_2Cl_2$): $\lambda_{max}$ (log $\varepsilon$)= 253 (3.85), 274 (3.96), 288 (4.08), 300 (4.17), 326 (4.61), 336 sh (4.65), 339 (4.66), 353 sh (4.21), 372 sh (3.92), 392 (4.06), 414 (4.08), 504 sh (2.57), 538 (2.63), 583 sh (2.48), 643 sh (1.91) nm; HRMS (ESI positive) calcd for $C_{14}H_{10}O_2$+$H^+$ 211.0754; found 211.0736. Anal. Calcd for $C_{14}H_{10}O_2$: C, 79.98; H, 4.79; found: C, 80.04; H, 4.92.

*4.1.2. 1,2-Dihydro-1-oxa-4-phenylbenz[a]azulen-2-one (**1b**).* A solution of 2-hydroxyazulene (**2a**) (148 mg, 1.03 mmol) and ethyl benzoylacetate (**2b**) (267 mg, 1.39 mmol) in 1,2-dichloroethane (15 mL) was refluxed for 15 h in the presence of aluminum chloride (296 mg, 2.22 mmol). The reaction mixture was poured into 2 M HCl solution and extracted with dichloromethane. The organic layer was washed with brine, dried over $MgSO_4$, and concentrated under reduced pressure. The residue was purified by column chromatography on silica gel with ethyl acetate/hexane (1:4) to afford **1b** (29 mg, 10%). Dark purple crystals; mp 158.0–159.4 °C (toluene); $^1$H NMR (500 MHz, $CDCl_3$): $\delta$=8.38 (d, 1H, *J*=10.0 Hz, 9-H), 7.89 (d, 1H, *J*=9.7 Hz, 5-H), 7.61 (dd, 1H, *J*=10.2, 9.4 Hz, 7-H), 7.58–7.51 (m, 5H, 4-Ph), 7.40 (dd, 1H, *J*=10.0, 9.4 Hz, 8-H), 7.17 (s, 1H, 10-H), 7.14 (dd, 1H, *J*=10.2, 9.7 Hz, 6-H), 6.08 (s, 1H, 3-H); $^{13}$C NMR (125 MHz, $CDCl_3$): $\delta$=162.88 (C-10a), 162.37 (C-2), 154.82 (C-4), 142.84 (C-9a), 137.17 (s, 4-Ph), 136.96 (C-9), 136.82 (C-7), 134.20 (C-5), 134.09 (C-4b), 129.43 (d, 4-Ph), 128.88 (d, 4-Ph), 127.83 (d, 4-Ph), 127.49 (C-8), 126.94 (C-6), 108.79 (C-3), 107.84 (C-4a), 103.88 (C-10); IR (KBr disk): $\nu_{max}$=3049 (w), 1723 (s), 1593 (w), 1578 (w), 1561 (m), 1514 (s), 1475 (m), 1450 (m), 1435 (w), 1399 (m), 1363 (w), 1304 (w), 1272 (w), 1222 (w), 1174 (w), 1071 (w), 972 (w), 931 (w), 875 (w), 852 (w), 829 (m), 787 (w), 769 (m), 705 (w), 684 (w), 639 (w), 624 (w) cm$^{-1}$; UV/Vis ($CH_2Cl_2$): $\lambda_{max}$ (log $\varepsilon$)=278 sh (4.10), 295 (4.22), 330 sh (4.42), 344 (4.52), 358 sh (4.27), 373 sh (3.96), 397 (4.06), 418 (4.05), 501 sh (2.75), 531 (2.76), 582 sh (2.62), 638 sh (2.23) nm; HRMS (ESI positive) calcd for $C_{19}H_{12}O_2$+$H^+$ 273.0911; found 273.0902. Anal. Calcd for $C_{19}H_{12}O_2 \cdot 1/3H_2O$: C, 82.00; H, 4.59; found: C, 82.35; H, 5.01.

*4.1.3. Ethyl 1,2-dihydro-4-methyl-1-oxa-2-oxobenz[a]azulene-10-carboxylate (**1c**).* A solution of ethyl 2-hydroxyazulene-1-carboxylate (**2b**) (219 mg, 1.01 mmol), ethyl acetoacetate (**3a**) (172 mg, 1.32 mmol), and aluminum chloride (281 mg, 2.11 mmol) in 1,2-dichloroethane (15 mL) was refluxed for 15 h. The reaction mixture was poured into 2 M HCl solution and extracted with dichloromethane. The organic layer was washed with brine, dried over $MgSO_4$, and concentrated under reduced pressure. The residue was purified by column chromatography on silica gel with ethyl acetate/hexane (1:2) to afford **1c** (33 mg, 12%). Reddish orange crystals; mp 219.4–222.9 °C (toluene); $^1$H NMR (500 MHz, $CDCl_3$): $\delta$=9.75 (d, 1H, *J*=10.2 Hz, 9-H), 8.83 (d, 1H, *J*=10.0 Hz, 5-H), 7.87 (dd, 1H, *J*=9.8, 9.6 Hz, 7-H), 7.72 (dd, 1H, *J*=10.2, 9.6 Hz, 8-H), 7.65 (dd, 1H, *J*=10.0, 9.8 Hz, 6-H), 6.06 (s, 1H, 3-H), 4.50 (q, 2H, *J*=7.1 Hz, 10-COOEt), 2.76 (s, 3H, 4-Me), 1.50 (t, 3H, *J*=7.1 Hz, 10-COOEt); $^{13}$C NMR (125 MHz, $CDCl_3$): $\delta$=163.99 (10-COOEt), 161.86 (C-10a), 161.30 (C-2), 151.53 (C-4), 143.27 (C-9a), 138.46 (C-7), 137.71 (C-9), 136.77 (C-4b), 134.93 (C-5), 131.44 (C-8), 129.85 (C-6), 110.09 (C-3), 108.68 (C-4a), 103.13 (C-10), 60.43 (10-COOEt), 22.29 (4-Me), 14.53 (10-COOEt); IR (KBr disk): $\nu_{max}$=2921 (w), 1729 (s), 1715 (s), 1683 (w), 1663 (m), 1586 (m), 1556 (w), 1523 (s), 1457 (s), 1414 (w), 1296 (w), 1253 (m), 1202 (m), 1172 (w), 1089 (m), 1034 (m), 932 (w), 892 (w), 861 (w), 785 (w) cm$^{-1}$; UV/Vis ($CH_2Cl_2$): $\lambda_{max}$ (log $\varepsilon$)=252 sh (4.10), 262 sh (3.98), 273 sh (3.85), 298 sh (4.34), 313 (4.57), 327 (4.64), 336 sh (4.63), 341 (4.67), 374 (3.92), 394 (3.96), 413 (4.64), 482 sh (2.83), 509 (2.88), 551 sh (2.74), 604 sh (2.17) nm; HRMS (ESI positive) calcd for $C_{17}H_{14}O_4$+$K^+$ 321.0524; found 321.0483; HRMS (ESI positive) calcd for $C_{17}H_{14}O_4$+$Na^+$ 305.0784; found 305.0753; HRMS (ESI positive) calcd for $C_{17}H_{14}O_4$+$H^+$ 283.0965; found 283.0951. Anal. Calcd for $C_{17}H_{14}O_4$: C, 72.33; H, 5.00; found: C, 72.16; H, 4.96.

*4.1.4. 10-Bromo-1,2-dihydro-4-methyl-1-oxabenz[a]azulen-2-one (**4**).* To a solution of 1,2-dihydro-4-methyl-1-oxabenz[*a*]azulen-2-one (**1a**) (40 mg, 0.19 mmol) in dichloromethane (2 mL) was added *N*-bromosuccinimide (NBS) (36 mg, 0.20 mmol) at room temperature. After the solution was stirred at the same temperature for 2.5 h, the reaction mixture was concentrated under reduced pressure. The residue was purified by column chromatography on silica gel with ethyl acetate/dichloromethane (1:2) to afford **4** (23 mg, 42%), 3,10-dibromo-1,2-dihydro-4-methyl-1-oxabenz[*a*]azulen-2-one (**5**) (22 mg, 31%), and the recovered **1a** (8.6 mg, 22%).

*Compound* **4**: Yellowish brown crystals; mp 189.1–189.4 °C (toluene); $^1$H NMR (500 MHz, $CDCl_3$): $\delta$=8.68 (d, 1H, *J*=9.7 Hz, 5-H),

8.45 (d, 1H, *J*=10.1 Hz, 9-H), 7.75 (dd, 1H, *J*=9.7, 9.7 Hz, 7-H), 7.52 (dd, 1H, *J*=10.1, 9.7 Hz, 8-H), 7.50 (dd, 1H, *J*=9.7, 9.7 Hz, 6-H), 6.05 (s, 1H, 3-H), 2.78 (s, 3H, 4-Me); $^{13}$C NMR (125 MHz, $CDCl_3$): $\delta$=161.21 (C-2), 158.92 (C-10a), 151.66 (C-4), 138.04 (C-9a), 137.55 (C-7), 135.35 (C-9), 134.08 (C-4b), 133.93 (C-5), 127.81 (C-8), 127.41 (C-6), 109.62 (C-3), 108.42 (C-4a), 91.22 (C-10), 21.88 (4-Me); IR (KBr disk): $\nu_{max}$=3062 (w), 2910 (w), 1733 (w), 1597 (m), 1579 (m), 1520 (s), 1486 (w), 1456 (m), 1444 (w), 1392 (m), 1374 (w), 1306 (w), 1283 (w), 1072 (w), 921 (w), 878 (m), 828 (w), 747 (m), 727 (w), 664 (w), 603 (w) cm$^{-1}$; UV/Vis ($CH_2Cl_2$): $\lambda_{max}$ (log $\varepsilon$)=260 (3.75), 276 (3.78), 293 sh (4.02), 306 sh (4.18), 330 (4.52), 342 sh (4.55), 343 (4.56), 359 sh (4.07), 382 (3.77), 402 (3.94), 423 (3.90), 517 sh (2.39), 546 (2.42), 593 sh (2.24), 652 sh (1.39) nm; HRMS (ESI positive) calcd for $C_{14}H_9BrO_2$+H$^+$ 288.9859; found 288.9852. Anal. Calcd for $C_{14}H_9BrO_2$: C, 58.16; H, 3.14; found: C, 58.35; H, 3.44.

*4.1.5. 3,10-Dibromo-1,2-dihydro-4-methyl-1-oxabenz[a]azulen-2-one (**5**).* To a solution of 1,2-dihydro-4-methyl-1-oxabenz[*a*]azulen-2-one (**1a**) (100 mg, 0.476 mmol) in dichloromethane (2.5 mL) was added *N*-bromosuccinimide (NBS) (175 mg, 0.983 mmol) at room temperature. After the solution was stirred at the same temperature for 1 h, the reaction mixture was poured into water and extracted with dichloromethane. The organic layer was washed with brine, dried over $MgSO_4$, and concentrated under reduced pressure. The residue was purified by column chromatography on silica gel with dichloromethane to afford **5** (159 mg, 91%). Brown crystals; mp 193.4–194.3 °C (toluene); $^1$H NMR (500 MHz, $CDCl_3$): $\delta$=8.80 (d, 1H, *J*=9.7 Hz, 5-H), 8.51 (d, 1H, *J*=10.3 Hz, 9-H), 7.80 (dd, 1H, *J*=10.2, 9.5 Hz, 7-H), 7.58 (dd, 1H, *J*=10.3, 9.5 Hz, 8-H), 7.56 (dd, 1H, *J*=10.2, 9.7 Hz, 6-H), 3.02 (s, 3H, 4-Me); IR (KBr disk): $\nu_{max}$=2921 (w), 1733 (s), 1599 (w), 1576 (m), 1546 (w), 1523 (s), 1473 (w), 1458 (w), 1438 (m), 1389 (m), 1371 (w), 1301 (w), 1252 (w), 1226 (w), 1076 (w), 1023 (w), 945 (m), 913 (w), 831 (w), 746 (m), 700 (w), 650 (w) cm$^{-1}$; UV/Vis ($CH_2Cl_2$): $\lambda_{max}$ (log $\varepsilon$)=267 (3.93), 281 (3.96), 299 sh (4.12), 312 (4.21), 339 (4.51), 349 sh (4.54), 352 (4.54), 366 sh (4.20), 391 sh (3.93), 411 (4.13), 434 (4.12), 519 sh (2.59), 542 (2.60), 599 sh (2.38), 661 sh (1.50) nm; HRMS (ESI positive) calcd for $C_{14}H_8Br_2O_2$+H$^+$ 366.8964; found 366.8937. Anal. Calcd for $C_{14}H_8Br_2O_2$: C, 45.69; H, 2.19; found: C, 45.96; H, 2.53. Low solubility hampered the measurement of $^{13}$C NMR.

*4.1.6. 1,2-Dihydro-4-methyl-1-oxa-2-oxobenz[a]azulene-10-carbaldehyde (**6**).* To a solution of 1,2-dihydro-4-methyl-1-oxabenz[*a*]azulen-2-one (**1a**) (108 mg, 0.514 mmol) in dimethylformamide (10 mL) was added phosphorus oxychloride (250 μl, 2.68 mmol) at room temperature. The resulting mixture was stirred at room temperature for 2 h. The reaction mixture was poured into water, made alkaline with 0.1 M NaOH, and then extracted with dichloromethane. The organic layer was washed with brine, dried with $MgSO_4$, and concentrated under reduced pressure. Hexane was added to the residue. The precipitated crystals were collected by filtration, washed with hexane, and dried in vacuo to afford **6** (96 mg, 78%). Reddish orange crystals; mp >350 °C (toluene); $^1$H NMR (500 MHz, $CDCl_3$): $\delta$=10.60 (s, 1H, 10-CHO), 9.92 (d, 1H, *J*=10.3 Hz, 9-H), 8.96 (d, 1H, *J*=10.0 Hz, 5-H), 7.98 (dd, 1H, *J*=9.7, 9.7 Hz, 7-H), 7.87 (dd, 1H, *J*=10.3, 9.7 Hz, 8-H), 7.79 (dd, 1H, *J*=10.0, 9.7 Hz, 6-H), 6.16 (d, 1H, *J*=1.1 Hz, 3-H), 2.83 (d, 3H, *J*=1.1 Hz, 4-Me); $^{13}$C NMR (125 MHz, $CDCl_3$): $\delta$=184.62 (10-CHO), 165.01 (C-10a), 160.70 (C-2), 152.01 (C-4), 141.96 (C-9a), 139.51 (C-7), 139.03 (C-9), 138.51 (C-4b), 135.94 (C-5), 134.02 (C-8), 131.45 (C-6), 110.36 (C-3), 110.07 (C-10), 108.75 (C-4a), 22.23 (4-Me); IR (KBr disk): $\nu_{max}$=2927 (w), 1733 (s), 1718 (w), 1650 (s), 1583 (m), 1524 (s), 1476 (w), 1455 (s), 1420 (w), 1399 (w), 1372 (m), 1314 (w), 1289 (w), 1197 (w), 1025 (m), 946 (w), 922 (w), 881 (m), 775 (w), 763 (w), 683 (w), 649 (w), 606 (w), 552 (w) cm$^{-1}$; UV/Vis ($CH_2Cl_2$): $\lambda_{max}$ (log $\varepsilon$)=253 sh (4.00), 259 (4.03), 270 (4.00), 324 sh (4.65), 330 (4.66), 341 sh (4.60), 345 (4.59), 380 sh (3.83), 404 (3.93), 422 (3.95), 483 sh (2.97), 504 (2.99), 545 sh (2.83), 599 sh (2.21) nm; HRMS (ESI positive) calcd for $C_{15}H_{10}O_3$+Na$^+$ 261.0522; found 261.0535; HRMS (ESI positive) calcd for $C_{15}H_{10}O_3$+H$^+$ 239.0703; found 239.0702. Anal. Calcd for $C_{15}H_{10}O_3$: C, 75.62; H, 4.23; found: C, 75.37; H, 4.23.

*4.1.7. 1,2-Dihydro-4-methyl-1-oxa-10-(trimethylsilylethynyl)benz[a]azulen-2-one (**7**).* To a solution of 10-bromo-1,2-dihydro-4-methyl-1-oxabenz[*a*]azulen-2-one (**4**) (16 mg, 0.055 mmol), trimethylsilylacetylene (315 μl, 2.23 mmol), CuI (5.1 mg, 0.027 mmol), and triethylamine (5 mL) in THF (10 mL) was added $Pd(Ph_3P)_4$ (14 mg, 0.012 mmol). The resulting mixture was stirred at 90 °C for 24 h in an autoclave. The reaction mixture was washed with 5% $NH_4Cl$ solution, dried over $MgSO_4$, and concentrated under reduced pressure. The residue was purified by column chromatography on silica gel with dichloromethane/hexane (3:1) and GPC with chloroform to afford **7** (8.0 mg, 47%) and the recovered **4** (1.4 mg, 9%). Brown crystals; mp 238.9–241.0 °C decomp. ($CH_2Cl_2$/hexane); $^1$H NMR (500 MHz, $CDCl_3$): $\delta$=8.71 (d, 1H, *J*=9.7 Hz, 5-H), 8.64 (d, 1H, *J*=10.2 Hz, 9-H), 7.76 (dd, 1H, *J*=10.0, 9.7 Hz, 7-H), 7.53 (dd, 1H, *J*=10.2, 9.7 Hz, 8-H), 7.51 (dd, 1H, *J*=10.0, 9.7 Hz, 6-H), 6.09 (d, 1H, *J*=1.0 Hz, 3-H), 2.79 (d, 3H, *J*=1.0 Hz, 4-Me), 0.35 (s, 9H, TMS); $^{13}$C NMR (125 MHz, $CDCl_3$): $\delta$=162.09 (C-10a), 161.66 (C-2), 151.73 (C-4), 143.62 (C-9a), 137.77 (C-7), 136.42 (C-9), 134.70 (C-4b), 134.23 (C-5), 128.36 (C-6 or C-8), 128.34 (C-6 or C-8), 119.06 (C-3), 108.35 (C-4a), 103.95 (C≡C), 98.30 (C-10), 95.24 (C≡C), 21.93 (4-Me), 0.22 (TMS); IR (KBr disk): $\nu_{max}$=2960 (m), 2901 (m), 2869 (w), 2142 (s, C≡C), 1735 (s, C=O), 1732 (s, C=O), 1637 (w), 1600 (s), 1583 (s), 1531 (s), 1471 (s), 1457 (s), 1452 (s), 1410 (s), 1401 (m), 1381 (w), 1325 (w), 1288 (m), 1246 (s), 1217 (w), 1179 (w), 1103 (m), 1022 (m), 991 (w), 930 (m), 926 (w), 883 (m), 856 (s), 841 (s), 821 (m), 765 (m), 755 (m), 733 (w), 718 (w), 695 (w), 653 (m), 603 (w), 575 (w), 557 (w), 502 (w) cm$^{-1}$; UV/Vis ($CH_2Cl_2$): $\lambda_{max}$ (log $\varepsilon$)=251 sh (4.24), 256 (4.24), 267 sh (4.14), 323 (4.57), 339 (4.62), 351 sh (4.62), 354 (4.63), 367 sh (4.09), 393 (3.85), 414 (3.99), 438 (3.91), 526 (2.54), 550 (2.54), 608 sh (2.28), 670 sh (1.50) nm; HRMS (MALDI-TOF, dithranol) calcd for $C_{19}H_{18}O_2Si$+H$^+$ 307.1149, found 307.1149; HRMS (MALDI-TOF, dithranol) calcd for $C_{19}H_{18}O_2Si^+$ 306.1071, found 306.1033. Anal. Calcd for $C_{19}H_{18}O_2Si$: C, 74.47; H, 5.92; found: C, 74.34; H, 5.78.

*4.1.8. 1,2-Dihydro-4-methyl-1-oxa-3,10-bis(trimethylsilylethynyl)benz[a]azulen-2-one (**8**).* To a solution of 3,10-dibromo-1,2-dihydro-4-methyl-1-oxabenz[*a*]azulen-2-one (**5**) (99 mg, 0.27 mmol), trimethylsilylacetylene (1.91 mL, 13.5 mmol), CuI (11 mg, 0.058 mmol), and triethylamine (10 mL) in THF (25 mL) was added $Pd(Ph_3P)_4$ (32 mg, 0.028 mmol). The resulting mixture was stirred at 90 °C for 24 h in an autoclave. The reaction mixture was washed with 5% $NH_4Cl$ solution, dried over $MgSO_4$, and concentrated under reduced pressure. The residue was purified by column chromatography on silica gel with dichloromethane/hexane (3:1) and GPC with chloroform to afford **8** (29 mg, 27%), 10-bromo-1,2-dihydro-4-methyl-1-oxabenz[*a*]azulen-2-one (**4**) (4.9 mg, 6%), and 1,2-dihydro-4-methyl-1-oxa-10-(trimethylsilylethynyl)benz[*a*]azulen-2-one (**7**) (44 mg, 53%).

*Compound* **8**: Yellowish brown crystals; mp 271.5–275.7 °C decomp. ($CH_2Cl_2$/hexane); $^1$H NMR (500 MHz, $CDCl_3$): $\delta$=8.78 (d, 1H, *J*=9.7 Hz, 5-H), 8.62 (d, 1H, *J*=10.1 Hz, 9-H), 7.78 (dd, 1H, *J*=10.2, 9.5 Hz, 7-H), 7.56 (dd, 1H, *J*=10.1, 9.5 Hz, 8-H), 7.54 (dd, 1H, *J*=10.2, 9.7 Hz, 6-H), 3.01 (s, 3H, 4-Me), 0.35 (s, 9H TMS), 0.31 (s, 9H, TMS); $^{13}$C NMR (125 MHz, $CDCl_3$): $\delta$=160.19 (C-2 or C-10a), 160.04 (C-2 or C-10a), 153.91 (C-4), 144.56 (C-9a), 138.34 (C-7), 136.43 (C-9), 134.95 (C-4b), 134.59 (C-5), 129.14 (C-6 or C-8), 129.08 (C-6 or C-8), 108.14 (C-4a), 105.27 (C-3), 104.44 (C≡C), 104.38 (C≡C), 98.98 (C≡C), 98.42 (C-10), 94.95 (C≡C), 19.98 (4-Me), 0.22 (TMS), 0.06 (TMS); IR (KBr disk): $\nu_{max}$=2959 (m), 2899 (m), 2871 (w), 2146 (s, C≡C), 1733 (s, C=O), 1628 (w), 1601 (m), 1581 (w), 1532 (s), 1487

(m), 1447 (s), 1405 (m), 1373 (w), 1325 (w), 1306 (w), 1284 (w), 1249 (s), 1211 (w), 1183 (w), 1132 (w), 1086 (m), 1008 (m), 946 (w), 930 (w), 858 (s), 843 (s), 763 (m), 706 (w), 668 (w), 618 (w), 567 (w) $cm^{-1}$; UV/Vis ($CH_2Cl_2$): $\lambda_{max}$ (log $\varepsilon$)=248 (4.51), 265 sh (4.33), 293 (4.23), 318 sh (4.28), 337 (4.45), 339 (4.45), 356 sh (4.51), 363 (4.54), 373 (4.54), 379 (4.54), 413 sh (4.08), 436 (4.25), 464 (4.27), 528 sh (2.88), 564 sh (2.82), 618 sh (2.54), 691 sh (1.68) nm; HRMS (MALDI-TOF, dithranol) calcd for $C_{24}H_{26}O_2Si_2+H^+$ 403.1544, found 403.1544; HRMS (MALDI-TOF, dithranol) calcd for $C_{24}H_{26}O_2Si_2^+$ 402.1466, found 402.1469. Anal. Calcd for $C_{24}H_{26}O_2Si_2$: C, 71.59; H, 6.51; found: C, 71.52; H, 6.50.

*4.1.9. 10-(2,2-Dibromoethenyl)-1,2-dihydro-4-methyl-1-oxabenz[a] azulen-2-one (**9**).* A mixture of 1,2-dihydro-4-methyl-1-oxabenz[*a*] azulen-2-one-10-carbaldehyde (**6**) (15 mg, 0.063 mmol), $CBr_4$ (218 mg, 0.657 mmol), and $Ph_3P$ (280 mg, 1.07 mmol) in 1,2-dichloroethane (10 mL) was stirred at 50 °C for 30 min under an Ar atmosphere. The reaction mixture was concentrated under reduced pressure. The residue was purified by column chromatography on silica gel with ethyl acetate/hexane (2:3) to afford **9** (12 mg, 48%). Reddish brown crystals; mp 170.4–173.7 °C decomp. ($CH_2Cl_2$/hexane); $^1H$ NMR (500 MHz, $CDCl_3$): $\delta$=8.79 (d, 1H, *J*=9.5 Hz, 5-H), 8.31 (d, 1H, *J*=10.2 Hz, 9-H), 7.82 (s, 1H, 1′-H), 7.79 (dd, 1H, *J*=10.1, 9.3 Hz, 7-H), 7.55 (dd, 1H, *J*=10.2, 9.3 Hz, 8-H), 7.54 (dd, 1H, *J*=10.1, 9.5 Hz, 6-H), 6.10 (d, 1H, *J*=1.0 Hz, 3-H), 2.82 (d, 3H, *J*=1.0 Hz, 4-Me); $^{13}C$ NMR (125 MHz, $CDCl_3$): $\delta$=161.74 (C-2), 159.42 (C-10a), 152.06 (C-4), 137.46 (C-7), 137.43 (C-9a), 135.86 (C-9), 135.19 (C-4b), 134.21 (C-5), 128.60 (C-1′), 127.89 (C-6), 127.83 (C-8), 110.96 (C-10), 109.42 (C-3), 108.52 (C-4a), 94.79 (C-2′), 22.04 (4-Me); IR (KBr disk): $\nu_{max}$=2924 (s), 2852 (m), 1732 (s, C=O), 1715 (s, C=O), 1628 (m), 1597 (m), 1583 (m), 1524 (s), 1479 (m), 1450 (s), 1406 (m), 1387 (w), 1372 (w), 1316 (w), 1292 (w), 1185 (w), 1106 (w), 1021 (w), 926 (w), 892 (w), 874 (w), 836 (m), 792 (w), 755 (m), 737 (w), 693 (w), 604 (w), 564 (w) $cm^{-1}$; UV/Vis ($CH_2Cl_2$): $\lambda_{max}$ (log $\varepsilon$)= 265 (4.10), 277 sh (4.03), 334 (4.63), 341 (4.63), 401 (3.98), 420 (3.96), 508 sh (2.58), 538 (2.60), 591 sh (2.41), 651 sh (1.85) nm; HRMS (MALDI-TOF, dithranol) calcd for $C_{16}H_{10}Br_2O_2+H^+$ 392.9120, found 392.9129. Anal. Calcd for $C_{16}H_{10}Br_2O_2$: C, 48.77; H, 2.56; found: C, 48.91; H, 2.75.

## Acknowledgements

This work was supported by JSPS KAKENHI Grant Numbers 21550031, 24550037 to S.I.

## Supplementary data

UV/Vis spectra of **1b** and **1c** and related compounds; cyclic voltammograms of **1a**; Copies of $^1H$ and $^{13}C$ NMR spectra of the reported compounds; DFT calculation results based on B3LYP/6-31G** method. Supplementary data related to this article can be found at http://dx.doi.org/10.1016/j.tet.2014.02.073.

## References and notes


1. Murray, R. D.; Mendez, J.; Brown, S. A. In *The Natural Coumarins: Occurrence, Chemistry and Biochemistry*; Murray, R. D. H., Mendez, J., Brown, S. A., Eds.; John Wiley: New York, NY, 1982.
2. Marumoto, S.; Miyazawa, M. *Tetrahedron* **2011**, *67*, 495–500.
3. Zhao, Y.; Zheng, Q.; Dakin, K.; Xu, K.; Martinez, M. L.; Li, W.-H. *J. Am. Chem. Soc.* **2004**, *126*, 4653–4663.
4. Lee, K.-S.; Kim, H.-J.; Kim, G.-H.; Shin, I.; Hong, J.-I. *Org. Lett.* **2008**, *10*, 49–51.
5. Ren, X.; Kondakova, M. E.; Giesen, D. J.; Rajeswaran, M.; Madaras, M.; Lenhart, W. C. *Inorg. Chem.* **2010**, *49*, 1301–1303.
6. Serin, J. M.; Brousmiche, D. W.; Fréchet, J. M. J. *J. Am. Chem. Soc.* **2002**, *124*, 11848–11849.
7. Kitamura, N.; Kohtani, S.; Nakagaki, R. *J. Photochem. Photobiol., C* **2005**, *6*, 168–185.
8. Iaroshenko, V. O.; Erben, F.; Mkrtchyan, S.; Hakobyan, A.; Vilches-Herrera, M.; Dudkin, S.; Bunescu, A.; Villinger, A.; Sosnovskikh, V. Y.; Langer, P. *Tetrahedron* **2011**, *67*, 7946–7955.
9. Goel, A.; Taneja, G.; Raghuvanshi, A.; Kant, R.; Maulik, P. R. *Org. Biomol. Chem.* **2013**, *11*, 5239–5253.
10. Zeller, K.-P. Azulene In. *Houben-Weyl; Methoden der Organischen Chemie*; Georg Thieme: Stuttgart, Germany, 1985; Vol. V, pp 127–418.
11. Ito, S.; Kubo, T.; Kondo, M.; Kabuto, C.; Morita, N.; Asao, T.; Fujimori, K.; Watanabe, M.; Harada, N.; Yasunami, M. *Org. Biomol. Chem.* **2003**, *1*, 2572–2580.
12. Shoji, T.; Shimomura, E.; Inoue, Y.; Maruyama, M.; Yamamoto, A.; Fujimori, K.; Ito, S.; Yasunami, M.; Morita, N. *Heterocycles* **2013**, *87*, 303–306.
13. Lin, B. B.; Morita, T.; Lin, Y.-S.; Chen, H.-L. *Bioorg. Med. Chem. Lett.* **2004**, *14*, 63–65.
14. Wakabayashi, H.; Yang, P. W.; Wu, C. P.; Shindo, K.; Ishikawa, S.; Nozoe, T. *Heterocycles* **1992**, *34*, 429–434.
15. Woodruff, E. H. *Organic Syntheses*, 1955, Collect. Vol. 3, pp 581–583.
16. Fischer, G. Azulenes Fused to Heterocycles In. *Advances in Heterocyclic Chemistry*; Elsevier: Leipzig, Germany, 2009; Vol. 97, pp 131–218.
17. Nozoe, T.; Kikuchi, K. *Bull. Chem. Soc. Jpn.* **1963**, *36*, 633–637.
18. Wang, D.-I.; Feng, S.-S.; Cui, Q.-T.; Yu, J.-Y. *Heterocycles* **2012**, *85*, 441–448.
19. Nozoe, T.; Takase, K.; Shimazaki, N. *Bull. Chem. Soc. Jpn.* **1964**, *37*, 1644–1648.
20. Takase, K.; Asao, T.; Nozoe, T. *J. Chem. Soc., Chem. Commun.* **1968**, 368–369.
21. Yokoyama, R.; Ito, S.; Watanabe, M.; Harada, N.; Kabuto, C.; Morita, N. *J. Chem. Soc., Perkin Trans. 1* **2001**, 2257–2261.
22. Koch, M.; Blacque, O.; Venkatesan, K. *Org. Lett.* **2012**, *14*, 1580–1583.
23. (a) Shoji, T.; Ito, S.; Toyota, K.; Yasunami, M.; Morita, N. *Chem.—Eur. J.* **2008**, *14*, 8398–8408; (b) Shoji, T.; Ito, S.; Toyota, K.; Yasunami, M.; Morita, N. *Eur. J. Org. Chem.* **2009**, 4316–4324; (c) Shoji, T.; Maruyama, M.; Ito, S.; Morita, N. *Bull. Chem. Soc. Jpn.* **2012**, *85*, 761–773; (d) Shoji, T.; Ito, S.; Okujima, T.; Morita, N. *Org. Biomol. Chem.* **2012**, *10*, 8308–8313; (e) Shoji, T.; Ito, S.; Okujima, T.; Morita, N. *Chem.—Eur. J.* **2013**, *19*, 5721–5730; (f) Shoji, T.; Shimomura, E.; Maruyama, M.; Ito, S.; Okujima, T.; Toyota, K.; Morita, N. *Eur. J. Org. Chem.* **2013**, 7785–7799; (g) Shoji, T.; Maruyama, M.; Shimomura, E.; Maruyama, A.; Ito, S.; Okujima, T.; Toyota, K.; Morita, N. *J. Org. Chem.* **2013**, *78*, 12513–12524.
24. (a) Ito, S.; Inabe, H.; Morita, N.; Tajiri, A. *Eur. J. Org. Chem.* **2004**, 1774–1780; (b) Shoji, T.; Ito, S.; Toyota, K.; Morita, N. *Tetrahedron Lett.* **2009**, *50*, 2825–2827; (c) Ito, S.; Iida, T.; Kawakami, J.; Okujima, T.; Morita, N. *Eur. J. Org. Chem.* **2009**, 5355–5364; (d) Shoji, T.; Ito, S.; Okujima, T.; Morita, N. *Eur. J. Org. Chem.* **2011**, 5134–5140; (e) Shoji, T.; Shimomura, E.; Maruyama, M.; Ito, S.; Okujima, T.; Morita, N. *Eur. J. Org. Chem.* **2013**, 957–964.
25. Ito, S.; Okujima, T.; Kabuto, C.; Morita, N. *Tetrahedron* **2003**, *59*, 4651–4659.
26. The B3LYP/6-31G** density functional calculations were performed by Spartan'10, Wavefunction: Irvine, CA.
27. Reddy, C. R.; Srikanth, B.; Rao, N. N.; Shin, D.-S. *Tetrahedron* **2008**, *64*, 11666–11672.